

# Transition of the Stellar Initial Mass Function Explored with Binary Population Synthesis

Takuma Suda<sup>1\*</sup>, Yutaka Komiya<sup>1</sup>, Shimako Yamada<sup>2</sup>, Yutaka Katsuta<sup>2</sup>, Wako Aoki<sup>1</sup>, Pilar Gil-Pons<sup>3</sup>, Carolyn L. Doherty<sup>4</sup>, Simon W. Campbell<sup>4</sup>, Peter R. Wood<sup>5</sup>, and Masayuki Y. Fujimoto<sup>6,7†</sup>

<sup>1</sup>*National Astronomical Observatory of Japan, Osawa 2-21-1, Mitaka, Tokyo 181-8588, Japan*

<sup>2</sup>*Department of Cosmoscience, Hokkaido University, Kita 10 Nishi 8, Kita-ku, Sapporo 060-0810, Japan*

<sup>3</sup>*Universitat Politècnica de Catalunya, Campus Baix Llobregat, Building C3, 08860 Castelldefels, Spain*

<sup>4</sup>*Monash Centre for Astrophysics (MoCA), Monash University, Victoria 3800, Australia*

<sup>5</sup>*Australian National University, Cotter Road, Weston Creek ACT 2611, Australia*

<sup>6</sup>*Nuclear Data Center, Hokkaido University, Kita 10 Nishi 8, Kita-ku, Sapporo 060-0810, Japan*

<sup>7</sup>*Faculty of Engineering, Hokkaido University, 4-1-40, Asahimachi, Toyohira-ku, Sapporo, 062-8605, Japan*

Accepted 1988 December 15. Received 1988 December 14; in original form 1988 October 11 ; draft version of 2013 February 11

## ABSTRACT

The stellar initial mass function (IMF) plays a crucial role in determining the number of surviving stars in galaxies, the chemical composition of the interstellar medium, and the distribution of light in galaxies. A key unsolved question is whether the IMF is universal in time and space. Here we use state-of-the-art results of stellar evolution to show that the IMF of our Galaxy made a transition from an IMF dominated by massive stars to the present-day IMF at an early phase of the Galaxy formation. Updated results from stellar evolution in a wide range of metallicities have been implemented in a binary population synthesis code, and compared with the observations of carbon-enhanced metal-poor (CEMP) stars in our Galaxy. We find that applying the present-day IMF to Galactic halo stars causes serious contradictions with four observable quantities connected with the evolution of AGB stars. Furthermore, a comparison between our calculations and the observations of CEMP stars may help us to constrain the transition metallicity for the IMF which we tentatively set at  $[\text{Fe}/\text{H}] \approx -2$ . A novelty of the current study is the inclusion of mass loss suppression in intermediate-mass AGB stars at low-metallicity. This significantly reduces the overproduction of nitrogen-enhanced stars that was a major problem in using the high-mass star dominated IMF in previous studies. Our results also demonstrate that the use of the present day IMF for all time in chemical evolution models results in the overproduction of Type I.5 supernovae. More data on stellar abundances will help to understand how the IMF has changed and what caused such a transition.

**Key words:** stars: evolution — stars: AGB and post-AGB — Galaxy: halo — binaries: general — stars: formation — stars: Population II

## 1 INTRODUCTION

The IMF is one of the most important factors influencing the evolution of galaxies. In particular, possible transitions of the stellar IMF from that of the first (metal-free) stars to that of the present-day (metal-rich) stars have been given much attention. The typical first generation stars are

thought to be predominantly of high-mass (e.g.  $\sim 40M_{\odot}$  according to Hosokawa et al. 2011) from studies of star formation in metal-free environments. However, the actual form of the IMF for such stars is poorly understood and is still controversial (see e.g. Greif et al. 2012, and references therein). In addition, there are few studies dealing with the transition of the IMF during the early epoch of the Galaxy. If the IMF is not universal then a question arises - how and when did the IMF change to the present-day IMF which is biased towards low-mass stars ( $< 0.8M_{\odot}$ ) (Salpeter 1955)?

\* E-mail: takuma.suda@nao.ac.jp

† visiting researcher

Extremely metal-poor stars (EMP stars) observed in the Galaxy can help to answer this question because we can estimate the number of former AGB stars that contributed to the change of the surface abundances evident in these stars. Spectroscopy of EMP stars (Beers & Christlieb 2005) reveals that carbon-enhanced stars are very common amongst EMP stars (20 % or more (Suda et al. 2011; Carollo et al. 2012)) when compared to the higher-metallicity subgiant CH stars ( $\sim 1$  %) (Luck & Bond 1991). The large frequency of carbon-enhanced metal-poor (CEMP) stars is argued to be a consequence of binary mass transfer from AGB stars that have undergone carbon dredge-up into their envelopes (Fujimoto et al. 2000; Suda et al. 2004; Lucatello et al. 2005b; Komiya et al. 2007). The mechanism for carbon enhancement, the third dredge-up (TDU), is the currently accepted theory that explains the origin of classical Ba II stars and CH stars (see, e.g. McClure & Woodsworth 1990). In the same manner, the origins of some CEMP stars are thought to be explained by the binary scenario, i.e., the observed stars have binary companions that are now unseen white dwarfs. One of the advantages of this scenario is that we do not expect all the observed EMP stars to show carbon enhancement on their surface. This is qualitatively consistent with the recent discovery of EMP stars in the lowest metallicity range without large enhancements of carbon (Caffau et al. 2011). Binarity has been statistically confirmed for the population of CEMP stars that show enhancements of *s*-process elements (Suda et al. 2004; Lucatello et al. 2005b), as is expected from theory. These objects are called CEMP-*s* stars, in contrast to the other subclass of CEMP stars, the CEMP-no stars, which do not show any enhancement of *s*-process elements. The origin of CEMP-no stars is still controversial (see, e.g., Norris et al. 2013). Observationally, there is another class of EMP stars that show enhancements of nitrogen greater than the enhancement of carbon. These stars are called nitrogen-enhanced metal-poor (NEMP) stars and are thought to be produced via binary mass transfer from intermediate-mass AGB stars which have converted C to N via hot bottom burning (HBB) during the AGB phase.

Previous works exploring the possibility that the IMF was different in the early universe (Lucatello et al. 2005a; Komiya et al. 2007) dealt only with the statistics of CEMP stars. (Komiya et al. (2009) also pointed out that the different IMF is suggested by the number of low-mass star survivors estimated from the survey areas of HK and Hamburg-ESO surveys.) In particular, the IMF which was proposed to have a peak at around  $10M_{\odot}$  (Komiya et al. 2007) has been criticized due to the possible overproduction of NEMP stars (Izzard et al. 2009; Pols et al. 2012). However recent work on pulsation driven mass loss in AGB stars at metallicities below  $[\text{Fe}/\text{H}] \sim -2.5$  (Wood 2011) suggests that NEMP star formation should have been suppressed in the early Universe. That study showed that the growth of pulsation during the AGB phase is too small to trigger dust-driven mass loss in low-metallicity, intermediate-mass stars. With mass-loss suppressed, the degenerate cores of these stars would have grown to be massive enough for the stars to explode as type I.5 supernovae, i.e., the mass of their cores would have grown to approach the Chandrasekhar mass limit (Arnett 1969; Iben & Renzini 1983). The purpose of this study is to explore the possibility that the IMF is different at low-

metallicity by including as many ingredients related to stellar evolution and binary evolution as possible. In particular, this is the first study to include characteristic AGB yields at  $[\text{Fe}/\text{H}] < -2.5$  (see, e.g., Fujimoto et al. 2000).

## 2 BINARY POPULATION SYNTHESIS OF EMP STARS: CODE DETAILS

We use the Monte Carlo method to simulate the evolution of binary systems by generating binaries with a range of initial primary mass, secondary mass, and binary period. The mass of the primary is described by a log-normal function or power-law function. The former is defined by  $dN/d\log m \propto \exp(-(\log(m/\mu))^2/(2\sigma^2))$ . The median mass and the dispersion are set at  $(\mu \text{ (in } M_{\odot}), \sigma) = (5, 0.6), (10, 0.4), (20, 0.45), (30, 0.5), \text{ and } (50, 0.6)$ , respectively, in order to reproduce CEMP-no/CEMP-*s* ratio following Komiya et al. (2007). Power-law functions are defined by  $dN/d\log m \propto m^{-x}$ , where we choose  $x = 1.35, 0.85, 0.35, \text{ and } 0.0$ . The lower and upper cut-off mass are set at  $0.08M_{\odot}$  and  $200M_{\odot}$ , respectively. The mass of the secondary is subject to the mass ratio function which was taken from the Duquennoy & Mayor (1991) or Raghavan et al. (2010). For the Raghavan et al. (2010) distribution we adopted a flat distribution by ignoring the preference for like-mass pairs. For the period distribution of binaries, we adopted a fitting formula for nearby main-sequence stars (Duquennoy & Mayor 1991; Raghavan et al. 2010; Rastegaev 2010).

The simulations generate binary systems for metallicities in the range  $-6 \leq [\text{Fe}/\text{H}] \leq -1$  in steps of 0.5 dex in each simulation. The total number of binary systems for a given metallicity is typically one million, which produces more than 1,000 observable giants. We note here that the simulations are compared to observations of giant stars (Figure 1). Giants were chosen so that the uncertainty concerning the depth of the convective envelopes for main-sequence stars is reduced, and because the uncertainty in the elemental abundances derived for dwarfs is considerable. We assume that the stars with  $M \geq 0.83M_{\odot}$  evolve to the final stage of their evolution.

In our simulations, we consider, for the first time, another channel of CEMP star formation, i.e., hydrogen ingestion into the helium flash convective zone for AGB stars at  $[\text{Fe}/\text{H}] \leq -2.5$  (He-Flash Driven Deep Mixing; He-FDDM) (Fujimoto et al. 1990, 2000). Previous studies have not taken this channel into account (Izzard et al. 2009; Pols et al. 2012). Surface chemical abundances of primary stars are taken from stellar models after the He-FDDM at the beginning of the thermally pulsing AGB (TP-AGB) phase (Suda & Fujimoto 2010), or after the TDU during the TP-AGB phase.

The surface abundance evolution for all the stars was taken from the literature (Suda & Fujimoto 2010; Karakas 2010; Gil-Pons & Doherty 2010; Gil-Pons et al. 2013). For models undergoing the He-FDDM event, we took the chemical abundances just after the dredge-up since this event dominates the change of the surface composition. For the TDU event, we took the average abundances of chemical yields provided by Karakas (2010). For models with  $[\text{Fe}/\text{H}] < -2.5$  with the mass range responsible for the TDU,

we adopted the same yields as in Karakas (2010) by adopting the values at  $[\text{Fe}/\text{H}] = -2.3$  of the same mass. We also considered the effect of carbon enhancement by super-AGB stars that host oxygen-neon-magnesium cores (Ritossa et al. 1999; Gil-Pons & Doherty 2010; Gil-Pons et al. 2013), although it turned out to be a minor contribution to CEMP stars in our simulations. A linear interpolation is made for the surface abundances between the model grids of initial mass and metallicity.

Binary mass transfer events are treated as instantaneous episodes. They are described by the masses of the binary components and the binary separation assuming Kepler rotation without any orbital ellipticity. If the binary separation is larger than the sum of the Roche radius of the primary star and the radius of the secondary star during the main sequence phase, wind accretion is assumed to be at play. Otherwise, Roche lobe overflow (RLOF) applies to the system. In this study, the occurrence of mass loss in AGB stars is controlled by a parameter introduced to take into account of the possible suppression of mass loss at low metallicity (Wood 2011). Here we assume that stars with  $5 < M/M_{\odot} < 8$  and  $[\text{Fe}/\text{H}] \leq -2.5$  do not eject any envelope and explode as Type I.5 supernovae, which is chosen to be consistent with the measured abundances using the SAGA database (Suda et al. 2008). The SAGA database includes 451 giant stars with carbon abundances derived from spectra with a resolution of  $R = \lambda/\Delta\lambda > 20000$ . The database covers the data published up to 2011 (August, 2012 update).

For wind accretion episodes we assume that the mass accretion onto the secondary star is subject to Bondi-Hoyle accretion with the constant stellar wind velocity of 20 km/s from the primary star. The amount of mass lost from the primary is estimated from initial-mass final-mass relations for white dwarfs (Han et al. 1994). These treatments are the same as in our previous work (Komiya et al. 2007) and the details are given in the reference (Komiya et al. 2007; Izzard et al. 2009; Eggleton 1983; Hurley et al. 2002).

For RLOF, the Roche radius is calculated from a commonly used approximation,  $R_1/a = 0.49q^{2/3}/(0.6q^{2/3} + \ln(1 + q^{1/3}))$ , where  $R_1$ ,  $a$ , and  $q = M_1/M_2$  are the radius of a primary, binary separation, and mass ratio, respectively, (Eggleton 1983). If the condition for RLOF accretion is satisfied, we assume a constant mass accretion of  $0.05M_{\odot}$  onto the secondary occurs, following Izzard et al. (2009). There is however no supporting evidence for this exact amount. An important point here is that the common envelope phase can be avoided only for binaries that have a mass ratio very close to unity. Thus the effect of RLOF accretion is actually always negligible in this study, and most binaries undergoing RLOF are excluded from the observable population due to merging.

The definition of CEMP giants is given by  $[\text{C}/\text{Fe}] \geq 0.7$  (Suda et al. 2011, see also Aoki et al. 2007) in the mass range 0.82 to  $0.83M_{\odot}$ , considering the stellar lifetimes in the Galactic halo population (comparable to the age of the Universe). Self-pollution by AGB stars is excluded due to their negligible contribution to the population compared with red giants. We designate CEMP star candidates as NEMP stars if the initial mass is in the range in which HBB operates. This mass range is a parameter of our model and is set at  $4.5 < M/M_{\odot} < 8$  in our fiducial models. For the definition of CEMP-*s* and CEMP-no stars, we use parameters for

mass and metallicity. We tentatively define a critical mass, set at  $3.5M_{\odot}$ , below (above) which the model stars become CEMP-*s* (no) stars during the AGB phase. For CEMP-no stars, it is required that the model stars should have  $[\text{Fe}/\text{H}] \leq -2.5$  to be consistent with observations. Note that the origin of CEMP-no stars is still controversial (see, e.g. Norris et al. 2013) and will be discussed in a separate paper. See also discussions in Suda et al. (2004) for more detail.

### 3 RESULTS AND DISCUSSION

The frequency of CEMP stars as a function of metallicity is given in Figure 1 for observations and for our models with different adopted IMFs. The CEMP fraction CEMP/EMP and the fractions CEMP-no/CEMP and NEMP/CEMP from our models are shown in Table 1 for a selected set of parameters. These ratios are averaged values from the SAGA database for metallicities below  $[\text{Fe}/\text{H}] = -2$ . They are obtained by taking a weighted average of the ratios in each of the metallicity bins below  $[\text{Fe}/\text{H}] = -2$ , with the weight being the number of stars in each bin. Model B is our fiducial model as it satisfactorily reproduces the observations. It was chosen to reproduce the distribution of carbon abundance as shown in Figure 2. It is to be noted that the CEMP fractions of stars taken from the SAGA database can be affected by selection bias, although they are consistent with the values derived for other homogeneous datasets (Yong et al. 2013; Carollo et al. 2012).

The results presented in the top panel of Fig. 1 demonstrate that the CEMP fraction for EMP stars is well reproduced by the high-mass star dominated IMF (model B), while the Salpeter IMF (model G) produces a very low CEMP fraction compared with observations. This is consistent with previous work (Izzard et al. 2009; Pols et al. 2012), although we note that those studies did not consider the effects of stellar evolution at  $[\text{Fe}/\text{H}] < -2.5$  and assumed that all the stars were born as binaries. The CEMP fraction produced by the model with the flat IMF (model J) is also below the observed value for  $[\text{Fe}/\text{H}] \leq -2$ . These results show that in order to reproduce the CEMP fraction at  $[\text{Fe}/\text{H}] \leq -2$ , the EMP population should be dominated by massive stars that end their lives as type II supernovae i.e. a high-mass star dominated IMF is required. For more metal-rich populations ( $[\text{Fe}/\text{H}] > -2$ ) such as the inner halo population, a flat IMF or low-mass star dominated IMF gives a better agreement with observations. This implies that an IMF transition occurred at  $[\text{Fe}/\text{H}] \sim -2$ , perhaps in association with the structure formation process of our Galaxy (see also Yamada et al. 2013). In the bottom panel of Fig. 1, we present a model with a transition of the IMF at  $[\text{Fe}/\text{H}] = -2$ .

Here we briefly mention the parameter dependencies of the simulations, although these are thoroughly discussed in a separate paper (Suda et al., in prep.). For the choice of the period distribution function, the distribution derived by Rastegaev (2010) gives preference to short period binaries, which results in efficient channels for the common envelope phase and CEMP star formation. We adopted this distribution because it is the only study that considers a population of metal-poor binary stars. Using the other two binary period distributions (Duquennoy & Mayor 1991; Raghavan et al. 2010) will decrease the fraction of CEMP

stars by up to  $\sim 10\%$  for the high-mass IMF and  $\sim 3\%$  for the low-mass IMF. Our fiducial model adopts other input physics and parameters so that the number of CEMP stars can be maximized with reasonable choices. The choice of the mass ratio function does not significantly alter the fraction of CEMP stars as discussed in Komiya et al. (2009) and Pols et al. (2012). The boundary masses for the occurrence of HBB and suppression of mass loss significantly affect the fraction of NEMP stars. These values are still open questions and cannot be determined at this stage (see Pols et al. 2012; Wood 2011). The mass boundary for the progenitors of CEMP-no stars is also an open question and can change the ratio CEMP-no/CEMP.

There are four observable constraints on the simulations. Three of them are shown in Table 1, and the other one is the  $[\alpha/\text{Fe}]$  abundances of EMP stars. Firstly, it can be seen that the CEMP fraction in our models can never reach as high as the observed 25 per cent when using a low-mass IMF (see also Fig. 1). In order to check the robustness of the conclusion, we have tested extreme assumptions for the model parameters, which include (1) a binary rate of 100 %, (2) excluding the contribution of supernova binaries because the speed of companion stars could have been higher than the velocity dispersion of the host halo after the disruption of binaries (Tauris & Takens 1998), and (3) the carbon abundance of primary star enhanced by a factor of 10. The superposition of all these assumptions still fails to explain the observed CEMP frequencies at low-metallicity when a low-mass IMF is used. A significant increase in the CEMP fraction can only be obtained by assuming that all the EMP stars are born as binary systems, although this gives the CEMP fraction well below 20 % at  $[\text{Fe}/\text{H}] = -2.5$ . A 100% binary fraction is however highly unlikely (Duquennoy & Mayor 1991; Raghavan et al. 2010; Rastegaev 2010).

Secondly, we find that the ratio CEMP-no/CEMP is extremely low for the models using the low-mass IMF. To obtain a ratio CEMP-no/CEMP = 0.5, we have to set the lower mass boundary for the formation of CEMP-no stars as small as  $\sim 1M_{\odot}$ . However, this then leads to a mismatch with the observed ratio CEMP-*s* /EMP. Thus it is evident that other sources of CEMP-no stars, for example stars that formed out of an ISM pre-enriched with carbon, are needed if we adopt a low-mass IMF (Meynet et al. 2010). We note however that any source of pre-enrichment would require more massive stars, i.e., a massive-star dominated IMF, although its shape depends on the efficiency of low-mass star formation out of ejecta from the massive stars.

Thirdly, the ratios of NEMP to CEMP stars in models with low-mass IMFs are too small to be compatible with the observations. The observed ratio is around  $\sim 0.1$  in the current available data (Suda et al. 2011; Pols et al. 2012), while it was previously thought to be much smaller (Johnson et al. 2007). The mass range of NEMP star progenitors would need to be  $2.5 \leq M/M_{\odot} \leq 8$ , without the assumption of mass loss suppression, to obtain a NEMP/CEMP ratio  $\sim 0.1$ . This mass range would need a higher efficiency of HBB at low metallicity as has been reported by some studies (Campbell & Lattanzio 2008). However, this range will also reduce the CEMP fraction dramatically, and hence cannot coexist with the requirement for the large frequency of CEMP stars.

Finally, the number of the progenitors of type I.5 supernovae dominates over, or is comparable to, that of type II supernovae when a low-mass IMF is used, which is not supported observationally since Galactic halo stars do not show the low values of  $[\alpha/\text{Fe}]$  that would be expected from type I.5 supernovae (Nomoto et al. 1984). Thus our simulations arrive at the robust conclusion that population simulations using low-mass IMFs cannot match the observational constraints given by Galactic EMP stars.

Our results add to previous evidence for a non-universality of the IMF. Other evidence comes from studies such as the population of white dwarfs (Adams & Laughlin 1996), those involving simulations of star formation (see, e.g. Larson 2005), and observations of early-type galaxies (see, e.g. van Dokkum 2008). Our study shows that the observed population in the Galactic halo can be explained by a transition of the IMF from one biased towards high masses to one biased toward lower masses at a metallicity of  $[\text{Fe}/\text{H}] \sim -2$ . We propose that the statistics of CEMP and NEMP stars in the entire range of metallicity in our Galaxy and dwarf galaxies in the local group should be investigated to reveal the star formation history of galaxies.

## 4 CONCLUSIONS

We have compared the results of our binary population synthesis model with the observations of metal-poor halo stars in the Galaxy. We find that a low-mass biased IMF, similar to the present one, is incompatible with the four observable quantities related to the CEMP subclasses. On the other hand, considering a high-mass biased IMF, together with the occurrence of SN I.5 in a certain mass and metallicity range (supported by recent simulations of pulsation-driven mass-loss in low metallicity stars), a more reasonable agreement between models and observations is found. Our results imply that the transition of the IMF occurred around a metallicity of  $[\text{Fe}/\text{H}] \sim -2$ , which should be tested by star formation theory and observations. These results also give important clues in the most metal poor regimes as to the mass and metallicity limits of stars that experience HBB, TDU and stellar winds, or that allow the formation of CEMP (*-s* and *-no*) stars, NEMP stars, SN I.5 and SNI. Our understanding of these limits has been traditionally hampered by the scarcity of observations. We hope these results can help to improve the understanding of the chemical evolution of our Galaxy.

## ACKNOWLEDGMENTS

The authors thank Daniela Carollo and David Yong for kindly providing the data of CEMP fraction. We also thank Takayuki Saitoh for useful comments and suggestions. This work has been supported by Grant-in-Aid for Scientific Research (18104003), from Japan Society of the Promotion of Science. T.S. acknowledges the support of the Institutional Program for Young Researchers Overseas Visits by JSPS, which enhanced the results and discussions in this work.

## REFERENCES

- Adams F. C., Laughlin G., 1996, *ApJ*, 468, 586
- Aoki W., Beers T. C., Christlieb N., Norris J. E., Ryan S. G., Tsangarides S., 2007, *ApJ*, 655, 492
- Arnett W. D., 1969, *Astrophys. Space. Sci.*, 5, 180
- Beers T. C., Christlieb N., 2005, *A&AR*, 43, 531
- Caffau E. et al., 2011, *Nat*, 477, 67
- Campbell S. W., Lattanzio J. C., 2008, *A&A*, 490, 769
- Carollo D. et al., 2012, *ApJ*, 744, 195
- Duquennoy A., Mayor M., 1991, *A&A*, 248, 485
- Eggleton P. P., 1983, *ApJ*, 268, 368
- Fujimoto M. Y., Iben Jr. I., Hollowell D., 1990, *ApJ*, 349, 580
- Fujimoto M. Y., Ikeda Y., Iben Jr. I., 2000, *ApJ*, 529, L25
- Gil-Pons P., Doherty C. L., 2010, *Mem. S. A. It.*, 81, 974
- Gil-Pons P. et al., 2013, submitted to *A&A*
- Greif T. H. et al., 2012, *MNRAS*, 424, 399
- Han Z., Podsiadlowski P., Eggleton P. P., 1994, *MNRAS*, 270, 121
- Hosokawa T., Omukai K., Yoshida N., Yorke H. W., 2011, *Science*, 334, 1250
- Hurley J. R., Tout C. A., Pols O. R., 2002, *MNRAS*, 329, 897
- Iben Jr. I., Renzini A., 1983, *A&AR*, 21, 271
- Izzard R. G., Glebbeek E., Stancliffe R. J., Pols O. R., 2009, *A&A*, 508, 1359
- Johnson J. A., Herwig F., Beers T. C., Christlieb N., 2007, *ApJ*, 658, 1203
- Karakas A. I., 2010, *MNRAS*, 403, 1413
- Komiya Y., Suda T., Fujimoto M. Y., 2009, *ApJ*, 694, 1577
- Komiya Y., Suda T., Minaguchi H., Shigeyama T., Aoki W., Fujimoto M. Y., 2007, *ApJ*, 658, 367
- Larson R. B., 2005, *MNRAS*, 359, 211
- Lucatello S., Gratton R. G., Beers T. C., Carretta E., 2005a, *ApJ*, 625, 833
- Lucatello S., Tsangarides S., Beers T. C., Carretta E., Gratton R. G., Ryan S. G., 2005b, *ApJ*, 625, 825
- Luck R. E., Bond H. E., 1991, *ApJS*, 77, 515
- McClure R. D., Woodsworth A. W., 1990, *ApJ*, 352, 709
- Meynet G. et al., 2010, *A&A*, 521, A30
- Nomoto K., Thielemann F.-K., Yokoi K., 1984, *ApJ*, 286, 644
- Norris J. E. et al., 2013, *ApJ*, 762, 28
- Pols O. R., Izzard R. G., Stancliffe R. J., Glebbeek E., 2012, *A&A*, 547, A76
- Raghavan D. et al., 2010, *ApJS*, 190, 1
- Rastegaev D. A., 2010, *AJ*, 140, 2013
- Ritossa C., García-Berro E., Iben Jr. I., 1999, *ApJ*, 515, 381
- Salpeter E. E., 1955, *ApJ*, 121, 161
- Suda T., Aikawa M., Machida M. N., Fujimoto M. Y., Iben Jr. I., 2004, *ApJ*, 611, 476
- Suda T., Fujimoto M. Y., 2010, *MNRAS*, 405, 177
- Suda T. et al., 2008, *PASJ*, 60, 1159
- Suda T. et al., 2011, *MNRAS*, 412, 843
- Tauris T. M., Takens R. J., 1998, *A&A*, 330, 1047
- van Dokkum P. G., 2008, *ApJ*, 674, 29
- Wood P. R., 2011, in *ASP Conference Series*, 451, 87 eds. Qain S., Leung K., Zhu L., Kwok S.
- Yamada S., Suda T., Komiya Y., Aoki W., Fujimoto M. Y., 2013, submitted to *MNRAS*
- Yong D. et al., 2013, *ApJ*, 762, 27

**Table 1.** Characteristics of simulated EMP stars with the different IMF

ID	$(\mu, \sigma)$ or $x$	$\frac{\text{CEMP}^d}{\text{EMP}}$	$\frac{\text{CEMP-no}^d}{\text{CEMP}}$	$\frac{\text{NEMP}^d}{\text{CEMP}}$
A	5, 0.6	0.19	0.10	0.036
B <sup>a</sup>	10, 0.4	0.28	0.24	0.089
C	20, 0.45	0.22	0.29	0.092
D	30, 0.5	0.19	0.29	0.104
E	50, 0.6	0.19	0.28	0.082
F <sup>b</sup>	0.79, 0.51	0.037	0.00	0.072
G <sup>c</sup>	1.35	0.08	0.02	0.010
H	0.85	0.10	0.02	0.013
I	0.35	0.12	0.04	0.016
J	0.0	0.14	0.07	0.032
Observed		0.25	0.5	$\sim 0.1$

<sup>a</sup> Komiya et al. (2007)<sup>b</sup> Lucatello et al. (2005a)<sup>c</sup> Salpeter (1955)<sup>d</sup> Averaged values considering the metallicity distribution function of the metal-poor stars for  $[\text{Fe}/\text{H}] \leq -2$ . See text.

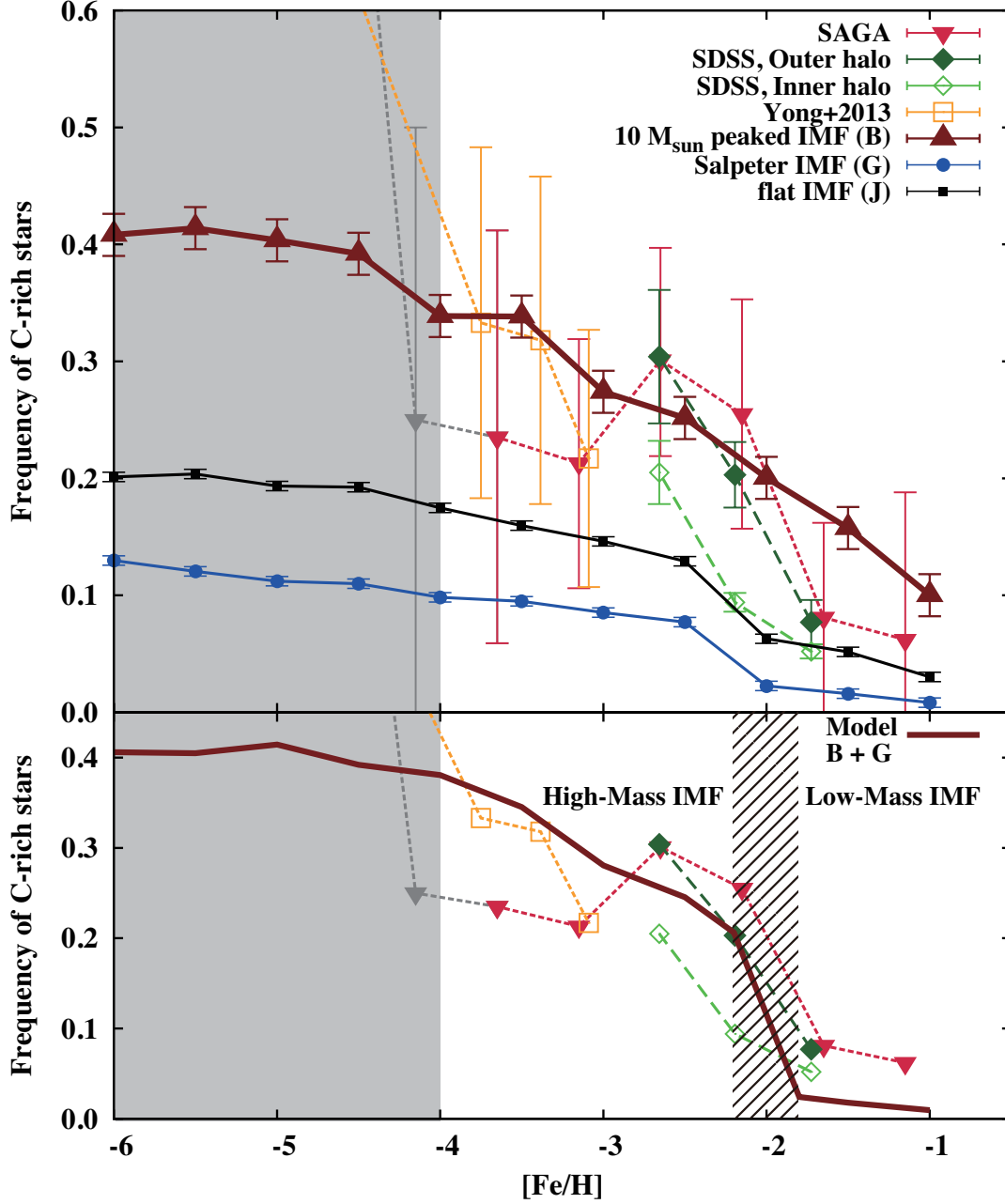


**Figure 1.** Top panel: the CEMP fraction CEMP/EMP for models with a log-normal IMF with the peak mass at  $10M_{\odot}$  (filled triangles, red), a flat IMF (filled squares, black), and a Salpeter IMF (filled circles, blue). The model names in the top-right corner correspond to those in Table 1. The observed CEMP fraction from the SAGA database (Suda et al. 2008) is shown by filled inverted triangles (red) and the observed CEMP fraction from Yong et al. (2013) is shown by open squares (orange). The CEMP fractions for the outer halo and the inner halo, kinematically selected from the SDSS sample (Carollo et al. 2012), are shown by filled and open diamonds, respectively (both green). The error bars for models and the SAGA sample are based on the bootstrap method with 1000 trials. For  $[\text{Fe}/\text{H}] \leq -4$  (shaded area), the number of stars in the observed sample is less than 10 in each bin and statistically unreliable. The criterion for CEMP stars is set at  $[\text{C}/\text{Fe}] \geq 0.7$  (Suda et al. 2011) for both models and observations. Bottom panel: the CEMP fractions for a model where the transition of the IMF at  $[\text{Fe}/\text{H}] = -2$  is taken into account by combining the results for the high-mass IMF (model B) and the low-mass IMF (model G). The combined model is compared with the same set of observations as in the top panel. The hatched area around  $[\text{Fe}/\text{H}] = -2$  represents the possible transition metallicity of the IMF from the high-mass star dominated IMF to the present-day IMF.

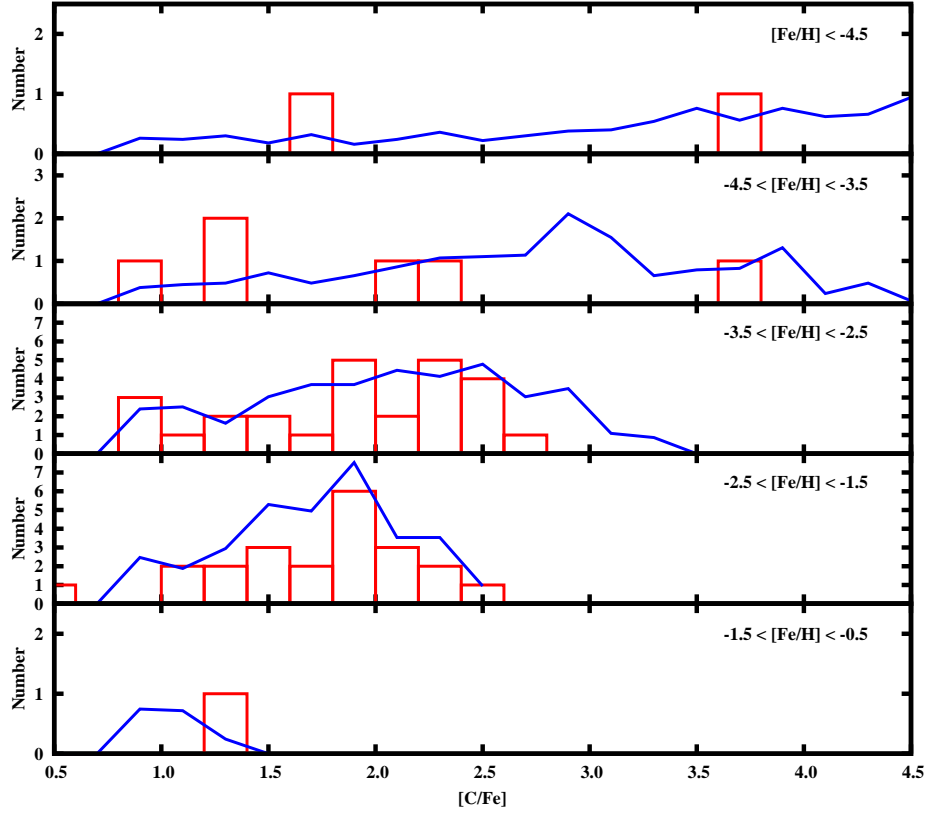


**Figure 2.** The comparison of the observed carbon abundance distribution and the distribution of carbon abundance for the fiducial model B. Histograms show the observed distributions for CEMP giants taken from the SAGA database, as used in Fig. 1. Model results are shown by solid lines where the number of stars is arbitrarily scaled.